# Influence of Small Molecules in Conducting Polyaniline on the Photovoltaic Properties of Solid-State Dye-Sensitized Solar Cells

**Shuxin Tan,[†] Jin Zhai,*[,†] Meixiang Wan,[†] Qingbo Meng,[‡] Yuliang Li,[†] Lei Jiang,[†] and Daoben Zhu[†]**

*Center for Molecular Science, Institute of Chemistry, and State Key Laboratory for Surface Physics, Institute of Physics, Chinese Academy of Sciences, Beijing 100080, People's Republic of China*

*Received: July 30, 2004; In Final Form: September 13, 2004*

Solid-state dye-sensitized solar cells (DSSCs) were fabricated using 4-dodecylbenzenesulfonic acid-doped polyaniline (PANI−DBSA) blended with LiI and 4-*tert*-butylpyridine (tBP) as hole conductors. The introduction of LiI and tBP into the polymer improves the photovoltaic behavior of solid-state DSSCs significantly. Compared with a DSSC only using PANI−DBSA as a hole conductor, one with LiI added at the optimum concentration gives an overall solar-to-electric energy conversion efficiency ($\eta_e$) increased by a factor of 5.13, whereas one with both LiI and tBP added at the optimum concentrations gives an $\eta_e$ increased by a factor of 6.6 and a maximum value of the incident photon to current conversion efficiency increased 100%. In addition, the photovoltage and photocurrent transients are determined to investigate the influence of LiI and tBP in PANI−DBSA on the photovoltaic performance of solid-state DSSCs.

## Introduction

In the system of dye-sensitized solar cells (DSSCs), the overall solar-to-electric conversion efficiency ($\eta_e$) with liquid electrolytes has already reached as high as 10%,[1,2] but it has technological problems such as device sealing and stability. Therefore, many studies have been done on solid- or quasi-solid-state hole transport materials for replacing the liquid electrolyte. For example, inorganic p-type semiconductors, the organic hole conducting material 2,2,7,7-tetrakis(*N*,*N*-di-*p*-methoxyphenylamino)-9,9-spirobifluorene, conducting polymers, room-temperature molten salts, and polymer gel electrolytes are all used for fabrication of DSSCs.[3−14] In the case of quasi-solid-state solar cells, though the $\eta_e$ approaches 7.0%,[11] the serious sealing problems still exist, while, in the case of solid-state solar cells, the maximum $\eta_e$ approaches 3%[3,4,14] with inorganic hole conductive materials, but these inorganic compounds are unstable and crystallize easily. Conducting polymers have also been studied as one kind of hole conductor,[6−9,15−19] but the $\eta_e$ and short-circuit current density ($I_{sc}$) are low. Therefore, finding a way to enhance the $\eta_e$ and $I_{sc}$ for solid-state DSSCs is of great importance. Lithium ions and 4-*tert*-butylpyridine (tBP) have already been used in the liquid electrolytes for improvement of the device performance,[2,20−22] and recently, they were also blended into solid-state hole conductors to enhance the photovoltaic behavior of the devices.[5,13,18]

In our previous study, a series of polyanilines (PANIs) were adopted as the hole conductors, and PANI doped with 4-dodecylbenzenesulfonic acid (PANI−DBSA) was found to be the optimum.[23] In this work, LiI and tBP were introduced into PANI−DBSA for fabrication of DSSCs, and the influence on the properties of the DSSCs was studied.

**CHART 1: Chemical Structure of PANI−DBSA**

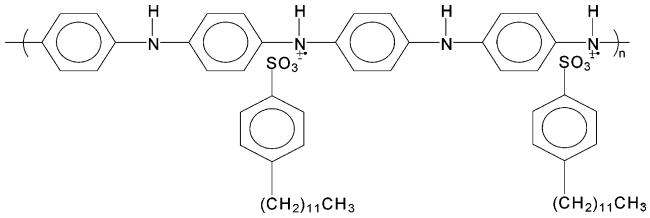


## Experimental Section

**Preparation of Hole Conductors.** PANI−DBSA was synthesized as previous reported,[24] and its chemical structure is given in Chart 1. The hole conductor matrix was prepared by adding LiI and tBP into a PANI−DBSA chloroform solution with vigorous stirring and then dried. The concentration of PANI−DBSA was 8.2 wt %.

**Preparation of Photoelectrodes and Solar Cells.** The fabrication of dye-sensitized $TiO_2$ photoelectrodes and solid-state DSSCs was reported elsewhere.[23] The specific surface area of $TiO_2$ electrodes was 20 $m^2/g$. To improve the electric contact, a graphite layer with a thickness of 10 $\mu$m was introduced between the hole conductor and the counter electrode.

**Measurements.** The photocurrent−voltage ($I-V$) characteristics and the photon-to-current conversion efficiency (IPCE) of the devices were obtained with an electrochemical analyzer (CHI630A, Chenhua Instruments Co., Shanghai) under solar simulator illumination (CMH-250, Aodite Photoelectronic Technology Ltd., Beijing). A GCR-4 Nd:YAG laser (Spectra Physics) was employed for transient photovoltage and photocurrent measurements. The laser pulse width was 6 ns. Transient photovoltage and photocurrent generation were recorded by a TDS3032 oscilloscope (Tektronix). The UV−vis spectra were measured by a spectrophotometer (U-3010, HITACHI). The Fourier transform infrared (FTIR) spectra were recorded in transmittance mode on a Bruker EQUINOX55 infrared spectrophotometer. Electrochemical impedance spectroscopy (EIS)

* To whom correspondence should be addressed. E-mail: zhaijin@iccas.ac.cn.

[†] Center for Molecular Science, Institute of Chemistry.

[‡] State Kay Laboratory for Surface Physics, Institute of Physics.

10.1021/jp046574y CCC: $27.50 
Published on Web 11/10/2004

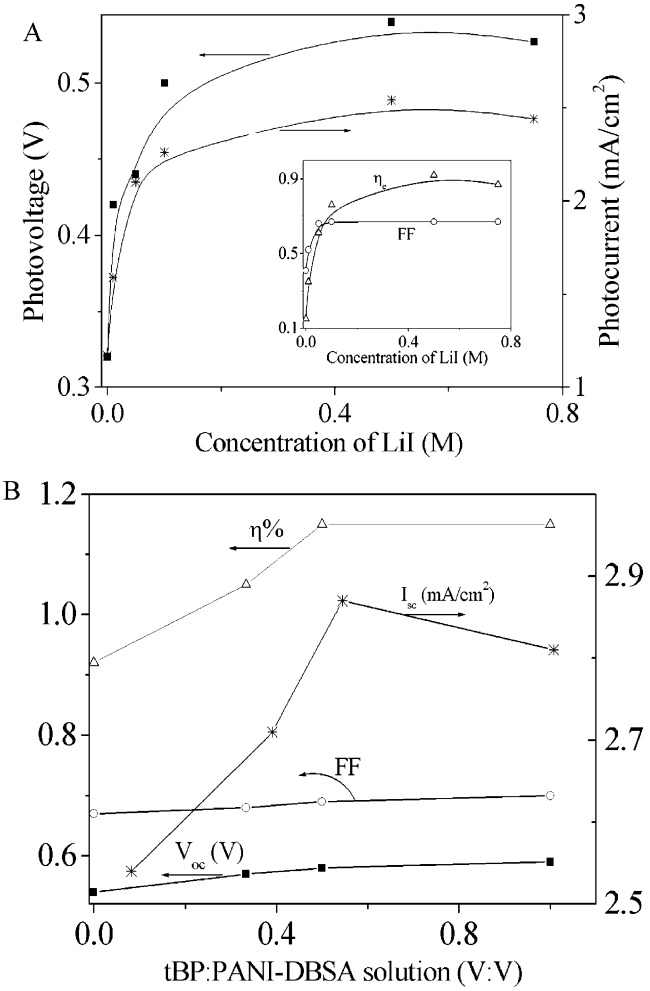


**Figure 1.** Relationships of $V_{oc}$, $I_{sc}$, FF, and $\eta_e$ with the concentrations of LiI (A) and tBP (B).

measurements of the PANI−DBSA film with and without LiI between two pieces of glass coated with fluorine-doped tin oxide (FTO) were performed with the Zahner IM6e impedance analyzer (Germany) in the frequency range from 0.1 Hz to 100 kHz, and the amplitude of the ac signal used was 2 mV without bias voltage. The impedance results in this paper are expressed as

$$Z = Z'/Z''$$

where $Z'$ and $Z''$ are the real part and the imaginary part of the impedance, respectively. Nyquist plots (plots of $Z''$ vs $Z'$) were drawn to analyze the impedance results.

## Results and Discussion

***I*−*V* Characteristics.** The relationships of open-circuit voltage ($V_{oc}$), short-circuit current density ($I_{sc}$), filling factor (FF), and overall solar-to-electrical energy conversion efficiency ($\eta_e$) with the concentration of LiI and tBP obtained from the *I*−*V* characteristics under 100 mW/cm$^2$ light intensity (Supporting Information) are presented in Figure 1. It can be seen that with increasing concentration of LiI, the photovoltaic properties of the devices are improved (Figure 1A), and the best performance of the device is achieved when the concentration of LiI is 0.5 M with a $V_{oc}$ of 0.54 V, an $I_{sc}$ of 2.54 mA/cm$^2$, an FF of 0.67, and an $\eta_e$ of 92%. Further increase of the LiI concentration leads to a decrease of the solar-to-electric energy conversion efficiency. The addition of tBP also improves the photovoltaic properties of the devices (Figure 1B). When the volume ratio of tBP to PANI−DBSA solution is 1:2, the best photovoltaic responses are obtained with a $V_{oc}$ of 0.58 V, an $I_{sc}$ of 2.87 mA/cm$^2$, an FF of 0.69, and an $\eta_e$ of 1.15%. Compared with a device only using PANI−DBSA as a hole conductor, one with LiI added at the proper concentration (0.5 M) gives increases in $V_{oc}$, $I_{sc}$, FF, and $\eta_e$ of 68%, 117%, 63%, and 513%, respectively, while one with tBP added at the optimum concentration ($V_{tBP}$: $V_{PANI-DBSA\ solution}$ = 1:2) gives increases of 81% in $V_{oc}$, 145% in $I_{sc}$, 68% in FF, and a factor of 6.6 in $\eta_e$. At the same time, the current−voltage characteristics of the devices with and without LiI and tBP at the optimum concentrations under dark conditions were also determined (Figure 2). It can be seen that the addition of LiI or both LiI and tBP decreases the dark current and shifts the onset potential of the dark current ca. 150 and 70 mV, respectively, which is one reason for the increase of FF and $V_{oc}$ in the presence of LiI and tBP.[18,20] All of these phenomena indicate that the introduction of LiI and tBP into PANI−DBSA can significantly improve the photovoltaic performance of such solid-state solar cells.

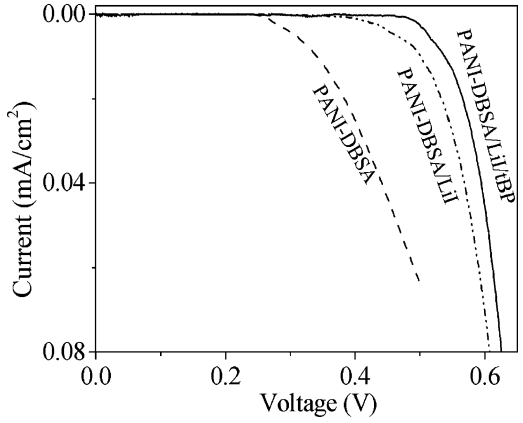


**Figure 2.** Current−voltage characteristics of the devices with the optimum concentrations of LiI and tBP and without them under dark conditions.

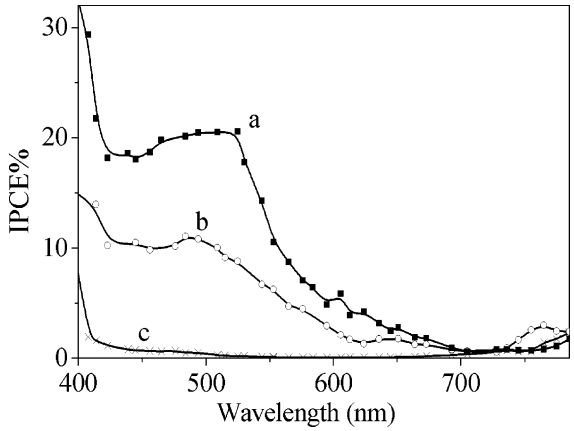


**Figure 3.** IPCE curves of the devices (the concentration of LiI in PANI−DBSA solution is 0.5 M, and the volume ratio of tBP to PANI−DBSA solution is 1:2): (a) dye-sensitized solar cell with both LiI and tBP in PANI−DBSA as the hole conductor; (b) dye-sensitized solar cell only with PANI−DBSA as the hole conductor; (c) heterojuction of FTO/$TiO_2$/PANI−DBSA−LiI−tBP/FTO without $N_3$ dye.

**IPCE.** Figure 3 displays IPCE curves of the solar cells. In the presence of both LiI and tBP at the optimum concentrations, values of the IPCE of more than 20% are obtained in a part of the visible region (Figure 3, curve a), which is mainly due to $N_3$ dye sensitization. For comparison, the IPCE curve of the $N_3$ dye-sensitized device only with PANI−DBSA as a hole

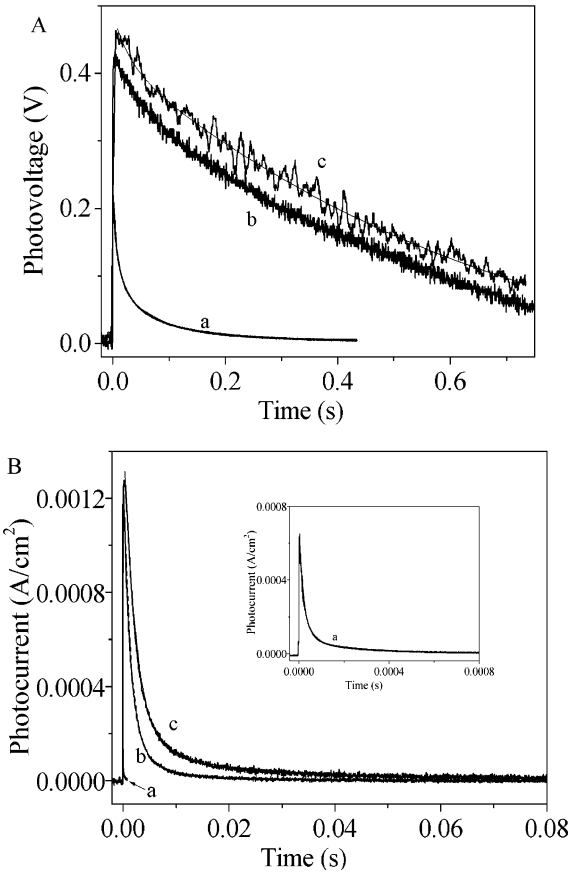


**Figure 4.** Photovoltage (A) and photocurrent (B) transients of the devices in the presence or absence of LiI and tBP (here, the concentrations of LiI and tBP are optimal). The inset in (B) shows the magnified photocurrent transient for the device with only PANI−DBSA as the hole conductor. (a)−(c) represent the device without LiI and tBP, with the addition of LiI, and in the presence of both LiI and tBP, respectively.

conductor is also displayed in Figure 3 (curve b). Obviously the values of IPCE in the presence of both LiI and tBP are all larger than those without LiI and tBP in the visible region from 400 to 700 nm, and at the absorption peak of the $N_3$ dye on the $TiO_2$ film, i.e., at about 500 nm, the value with the addition of both LiI and tBP (21%) is about twice as large as that without them (11%), which demonstrates that LiI and tBP is of great importance to improve the performance of the device. Moreover, at wavelengths longer than 700 nm, an obvious photocurrent response of the $N_3$ dye-sensitized device is observed when both LiI and tBP are added, which is similar to that of the heterojunction of FTO/$TiO_2$/PANI−DBSA−LiI−tBP/FTO without $N_3$ dye (Figure 3, curve c), indicating that the hole conductor matrix also can sensitize $TiO_2$.

**Transient Photovoltage and Photocurrent Measurements.** To study charge transport and recombination in DSSCs, the photovoltage and photocurrent transients for the devices with and without LiI and tBP (here, the concentrations of LiI and tBP are optimal) were measured (Figure 4). At the moment the dye was excited, the photocurrent and photovoltage responses in all devices instantaneously reached maxima; however, the peak values and the decay rates are different. The peak values of the device in the presence of both LiI and tBP are the largest, while they are the smallest without LiI and tBP. The decays in the photocurrent transients of all the devices are double-exponential, but the decay in the open-circuit photovoltage transient is single-exponential for the device in the presence of LiI and tBP and double-exponential for the device without LiI and tBP. For the double-exponential fits, the two exponential time constants differ by at least a factor of 6, and the faster decay accounts for about 60−90% of the whole decay. To avoid undue complexity, a transit time, $\tau_{1/2}$, is defined and discussed as the time when the photovoltage or photocurrent decays to half of the peak value. For the device without LiI and tBP, $\tau_{1/2}{}^V = 8.14$ ms and $\tau_{1/2}{}^I = 18.6$ $\mu$s (here $\tau_{1/2}{}^V$ and $\tau_{1/2}{}^I$ are referred as $\tau_{1/2}$ in the photovoltage and photocurrent transients, respectively). When LiI is added at the optimum concentration, $\tau_{1/2}{}^V$ and $\tau_{1/2}{}^I$ increase by factors of 32.6 and 64.0 compared with those without LiI. In the presence of both LiI and tBP at the optimum concentrations, $\tau_{1/2}{}^V$ and $\tau_{1/2}{}^I$ increase by factors of 1.23 and 1.93 relative to those with only the addition of LiI. The charge transport and recombination are considered to be similar in the dye-sensitized photoelectrodes and the counter electrodes in these devices because the corresponding materials and preparation process are the same. So the increase of $\tau_{1/2}{}^V$ indicates that LiI and tBP inhibit the interfacial charge recombination of injected electrons with dye cations or hole conductors. Meanwhile the increase of $\tau_{1/2}{}^I$ is larger than that of $\tau_{1/2}{}^V$, which means that LiI and tBP not only encumber the interfacial charge recombination, but also benefit charge transport in the hole conductor. Additionally, in the case of the same device, the decay of the photocurrent is faster than that of the photovoltage, which is due to the Fermi level gradient caused by ununiform electron distribution in the electrode under closed-circuit conditions[25,26] and charge losses in hole conductors and the external circuit.

In the liquid solar cell, lithium ions and tBP are usually used in the electrolyte, and the best performance of the photoelectric conversion has been achieved. Several studies suggested[21,27−32] that because the recombination rate of injected photoelectrons with oxidized dye and $I_3^-$ is much lower than both the regeneration rate of the dye by $I^-$ and the re-reduction rate of $I^-$ by electrons from the external circuit, the charge recombination with a liquid electrolyte is reduced considerably. Additionally, both the mobile carriers and the negative charges of the redox couple $I^-/I_3^-$ can screen photoelectrons and holes from each other in a liquid electrolyte and inhibit the recombination of $I_3^-$ with photoelectrons. Therefore, in the liquid solar cell, the interfacial recombination can be neglected.[20−22,27−32] A model for the effect of lithium ions and tBP on the liquid solar cell[20−22,30−32] is proposed in which the lithium ions and tBP have little effect on the interfacial recombination. Lithium ions increase the $I_{sc}$ and $\eta_e$ because they can shift the conduction band/trap state of $TiO_2$ away from the vacuum level and cause the interfacial electron transfer to be energetically more favorable,[22,30,31] while tBP enhances $V_{oc}$ and $\eta_e$ because it shifts the conduction band/trap state of $TiO_2$ opposite that of the lithium ions and suppresses the dark current at the semiconductor/electrolyte junction.[20,21,30,31] In a solid-state solar cell, the hole conductor does not possess the above-mentioned merits that the liquid electrolyte has. Bach et al. proposed that the main loss mechanism in the solid-state solar cell is the interfacial charge recombination.[33] Krüger and co-workers suggested[13] that, different from the liquid devices, in which the space charge layer is confined to a very thin layer at the interface because of the screen of the mobile electrolyte, in the solid device the space charge layer can be formed at the interface due to photoinduced charge injection, which can promote the recombination of injected electrons with a hole conductor cation. So, $Li^+$ enhances the photovoltaic performance of the device by altering the space charge layer and inhibiting the charge recombination. In this case, the influence of LiI and tBP is to inhibit interfacial charge

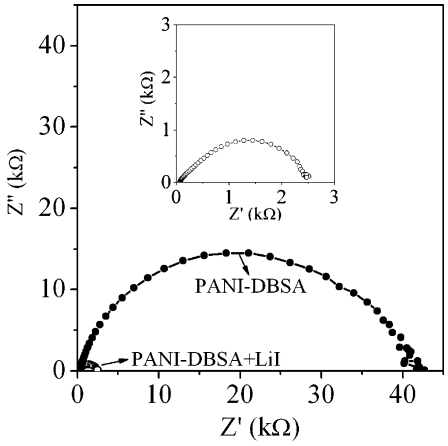


**Figure 5.** Nyquist plots of FTO/PANI−DBSA/FTO and FTO/PANI−DBSA−LiI/FTO. The inset shows the magnified Nyquist plot of FTO/PANI−DBSA−LiI/FTO.

recombination and suppress the dark current illustrated by photovoltage/photocurrent transients and dark current−voltage characteristics.

On the other hand, the photocurrent transients also show that the addition of LiI benefits charge transport in the hole conductor, which is consistent with the results obtained by EIS spectra (Figure 5) simultaneously. From Figure 5, it can be obviously observed that the resistance of PANI−DBSA in the presence of LiI decreases to one tenth of that of pure PANI−DBSA, illustrating that the addition of LiI enhances the conductivity of the polymer significantly. The Nyquist plots (EIS spectra) of both polymers with and without LiI (Figure 5) exhibit flattened semicircular characteristics in the measured range of frequency without linear behavior in the low-frequency range, which indicates that the controlling step in the electrode reaction is charge transfer, but not ionic diffusion.[34−38] This suggests that the conductivity of polymers in the presence or absence of LiI comes from charge transport but not ionic conductivity; therefore, similar to the pure PANI−DBSA, PANI−DBSA-doped LiI is believed to show hole mobility and can be used as a hole conductor material. In addition, the semicircles in the Nyquist plots are flattened and seem to be rotated clockwise around the origin by a certain angle because of the inhomogeneous electric field caused by the rough surface and porosity of the polymer films.[34−36] All of these indicate that PANI−DBSA has an interaction with LiI. This kind of interaction also can be reflected by the UV−vis and FTIR spectra. Figure 6A shows the UV−vis spectra of the PANI−DBSA film with and without LiI. For the PANI−DBSA film, the peak in the ultravisible region can be assigned to the $\pi-\pi$ electric transition in the conjugated benzene ring of the PANI−DBSA chain, and the peak at a wavelength of 780 nm is the absorption of polarons.[24] When LiI is added, the maximum absorption of the PANI−DBSA main chain remains at the same position. However, the peak of polarons shifts to 880 nm. The FTIR spectra are shown in Figure 6B. The broad bands close to 1480 and 1560 $cm^{-1}$, attributed to C═C stretching of the benzenoid and quinoid rings, all exist in PANI−DBSA with and without LiI. The difference is that the characteristic peaks of doping-state PANI shift from 1242 and 1126 $cm^{-1}$ to shorter wavelength numbers of 1220 and 1120 $cm^{-1}$,[24] respectively, which is consistent with their UV−vis spectra. All this evidence suggests that there is an interaction between LiI and PANI−DBSA, which results in a decrease of resistance, and thus benefits the photoelectric conversion properties of the solar cell.

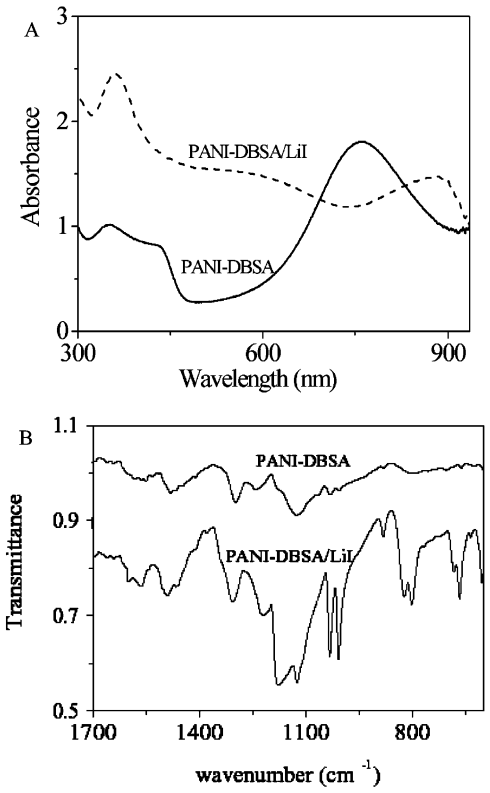


**Figure 6.** UV−vis (A) and FTIR (B) spectra of the PANI−DBSA films with and without LiI.

Additionally, the combination of tBP in the hole conductor increases the solubility of LiI in PANI−DBSA solution, which will reduce the phase separation and lead to a more homogeneous hole conductor film. As a result, the wetting of the $TiO_2$ film with the hole conductor is improved and the device performance is enhanced.

## Conclusion

The hole conductor of PANI−DBSA with LiI and tBP is effective as the hole conductor matrix for fabrication of a dye-sensitized $TiO_2$ solar cell, and the value of the conversion efficiency is 1.15%. Inhibition of the interfacial charge recombination, improvement of the wetting of the $TiO_2$ film, and the interaction with PANI−DBSA are reasons for the addition of lithium ion and tBP to enhance the device performance. This concept of a cooperative effect is considered to be significant for promoting practical application of the conductive polymers in the dye-sensitized $TiO_2$ solar cell, and can be extended to other systems, such as Lewis acids and bases (e.g., $Na^+$ and $K^+$), pyridine, polythiophene, polypyrrole, their derivatives, etc. An appropriate hole conductor matrix will be expected to further improve the performance of the dye-sensitized $TiO_2$ solar cell.

**Acknowledgment.** This work was supported by the State Key Project for Fundamental Research (Grant G1999064504), the Hi-Tech Research and Development program of China (863 project, Grant 2002AA302403), and the Special Research Foundation of the National Natural Science Foundation of China (Grant 20125102). We thank Prof. Xicheng Ai and Dr. Bin Liao at the Institute of Chemistry, Chinese Academy of Sciences, for their help in the photovoltage/photocurrent transient experiments and Yongfang Li and Chunhe Yang at the Institute of Chemistry, Chinese Academy of Sciences, for assisting us in the EIS experiments. We also thank Prof. A. Fujishima at the University of Tokyo, Japan, for their warmhearted help.

**Supporting Information Available:** Figure showing the $I-V$ characteristics of devices with different concentrations of LiI and different amounts of tBP (PDF). This material is available free of charge via the Internet at http://pubs.acs.org.

## References and Notes


(1) O'Regan, B.; Grätzel, M. *Nature* **1991**, *353*, 737.

(2) Nazeeruddin, M. K.; Pechy, P.; Renouard, T.; Zakeeruddin, S. M.; Hurnphry-Baker, R.; Comte, P.; Liska, P.; Cevery, L.; Costa, E.; Shklover, V.; Spiccia, L.; Deacon, G. B.; Bignozzi, C. A.; Grätzel, M. *J. Am. Chem. Soc.* **2001**, *123*, 1613.

(3) Kumara, G. R. R. A.; Konno, A.; Shiratsuchi, K.; Tsukahara, J.; Tennakone, K. *Chem. Mater.* **2002**, *14*, 954.

(4) Meng, Q.-B.; Takahashi, K.; Zhang, X.-T.; Sutanto, I.; Rao, T. N.; Sato, O.; Fujishima, A.; Watanabe, H.; Nakamori, T.; Uragami, M. *Langmuir* **2003**, *19*, 3572.

(5) Bach, U.; Lupo, D.; Comte, P.; Moser, J. E.; Weissörtel, F.; Salbeck, J.; Spreitzer, H.; Grätzel, M. *Nature* **1998**, *395*, 583.

(6) Gebeyehu, D.; Brabec, C. J.; Sariciftci, N. S.; Vangeneugden, D.; Kiebooms, R.; Vanderzande, D.; Kienberger, F.; Schindler, H. *Synth. Met.* **2002**, *125*, 279.

(7) Gebeyehu, D.; Brabec, C. J.; Sariciftci, N. S. *Thin Solid Films* **2002**, *403*−*404*, 271.

(8) Spiekermann, S.; Smestad, G.; Kowalik, J.; Tolbert, L. M.; Grätzel, M. *Synth. Met.* **2001**, *121*, 1603.

(9) Murakoshi, K.; Kogure, R.; Wada, Y.; Yanagida, S. *Sol. Energy Mater. Sol. Cells* **1998**, *55*, 113.

(10) Kubo, W.; Kitamura, T.; Hanabusa, K.; Wada, Y.; Yanagida, S. *Chem. Commun.* **2002**, 374.

(11) Wang, P.; Zakeeruddin, S. M.; Comte, P.; Exnar, I.; Grätzel, M. *J. Am. Chem. Soc.* **2003**, *125*, 1166.

(12) Stergiopoulos, T.; Arabatzis, I. M.; Katsaros, G.; Falaras, P. *Nano. Lett.* **2002**, *2*, 1259.

(13) Krüger, J.; Plass, R.; Cevey, L.; Piccirelli, M.; Grätzel, M.; Bach, U. *Appl. Phys. Lett.* **2001**, *79*, 2085.

(14) Kumara, G. R. R. A.; Kaneko, S.; Okuya, M.; Tennakone, K. *Langmuir* **2002**, *18* (26), 10493.

(15) Gebeyehu, D.; Brabec, C. J.; Padinger, F.; Fromherz, T.; Spiekermann, S.; Vlachopoulos, N.; Kienberger, F.; Schindler, H.; Sariciftci, N. S. *Synth. Met.* **2001**, *121*, 1549.

(16) Thelakkt, M.; Hagen, J.; Haarer, D.; Schmidt, H.-W. *Synth. Met.* **1999**, *102*, 1125.

(17) Smestad, G. P.; Spiekermann, S.; Kowalik, J.; Grant, C. D.; Schwartzberg, A. M.; Zhang, J.; Tolbert, L. M.; Moons, E. *Sol. Energy Mater. Sol. Cells* **2003**, *76*, 85.

(18) Saito, Y.; Kitamura, T.; Wada, Y.; Yanagida, S. *Synth. Met.* **2002**, *131*, 185.

(19) Arango, A. C.; Johnson, L. R.; Bliznyuk, V. N.; Schlesinger, Z.; Carter, S. A.; Hörhold, H.-H. *Adv. Mater.* **2000**, *12*, 1689.

(20) Nazeeruddin, M. K.; Kay, A.; Rodicio, I.; Humphry-Baker, R.; Müller, E.; Liska, P.; Vlachopoulos, N.; Grätzel, M. *J. Am. Chem. Soc.* **1993**, *115*, 6382.

(21) Huang, S. Y.; Schlichthörl, G.; Nozik, A. J.; Grätzel, M.; Frank, A. J. *J. Phys. Chem. B* **1997**, *101*, 2576.

(22) Kelly, C. A.; Farzad, F.; Thompson, D. W.; Stipkala, J. M.; Meyer, G. J. *Langmuir* **1999**, *15*, 7047.

(23) Tan, S.; Zhai, J.; Wan, M. X.; Meng, Q.; Li, Y.; Jiang, L.; Zhu, D. *Langmuir* **2004**, *20*, 2934.

(24) Li, Y.; Wan, M. *J. Funct. Polym.* **1998**, *11*, 337.

(25) Nakade, S.; Saito, Y.; Kubo, W.; Kanzaki, T.; Kitamura, T.; Wada, Y.; Yanagida, S. *J. Phys. Chem. B* **2004**, *108*, 1628.

(26) O'Regan, B. C.; Lenzmann, F. *J. Phys. Chem. B* **2004**, *108*, 4342.

(27) Gregg, B.-A.; Pichot, F.; Ferrere, S.; Fields, C. L. *J. Phys. Chem. B* **2001**, *105*, 1422.

(28) Schwarzburg, K.; Willig, F. *J. Phys. Chem. B* **1999**, *103*, 5743.

(29) Nogueira, A. F.; Durrant, J. R.; De Paoli, M.-A. *Adv. Mater.* **2001**, *13*, 826.

(30) Haque, S. A.; Tachibana, Y.; Willis, R. L.; Moser, J. E.; Grätzel, M.; Klug, D. R.; Durrant, J. R. *J. Phys. Chem. B* **2000**, *104*, 538.

(31) Redmond, C.; Fitzmaurice, D. *J. Phys. Chem.* **1993**, *97*, 1426.

(32) Schlichthörl, G.; Huang, S. Y.; Sprague, J.; Frank, A. J. *J. Phys. Chem. B* **1997**, *101*, 8141.

(33) Bach, U.; Kruger, J.; Grätzel, M. *Organic Photovoltaics*; SPIE—The International Society for Optical Engineering: San Diego, CA, 2000; Vol. 4108, p 1.

(34) Wu, H.; Li, Y. *Electrochemical Kinetics*; China High Education Press: Beijing; Springer-Verlag: Berlin, Heidelberg, 1998.

(35) Iseki, S.; Ohashi, K.; Nagaura, S. *Electrochim. Acta* **1972**, *17*, 2249.

(36) Zine, N.; Bausells, J.; Ivorra, A.; Aguiló, J.; Zabala, M.; Teixidor, F.; Masalles, C.; Viñas, C.; Errachid, A. *Sens. Actuators, B* **2003**, *91*, 76.

(37) Lindfors, T.; Ivaska, A. *Anal. Chim. Acta* **2000**, *404*, 111.

(38) Wang, F.; Lai, Y.-H.; Han, M.-Y. *Macromolecules* **2004**, *37*, 3222.